Simultaneous MR/PET – Clinical Reality?

Nina Schwenzer; Christina Pfannenberg; Holger Schmidt; Bernd Pichler; Claus D. Claussen

University of Tübingen, Department of Diagnostic and Interventional Radiology and Department of Preclinical Imaging and Radiopharmacy, Tübingen, Germany

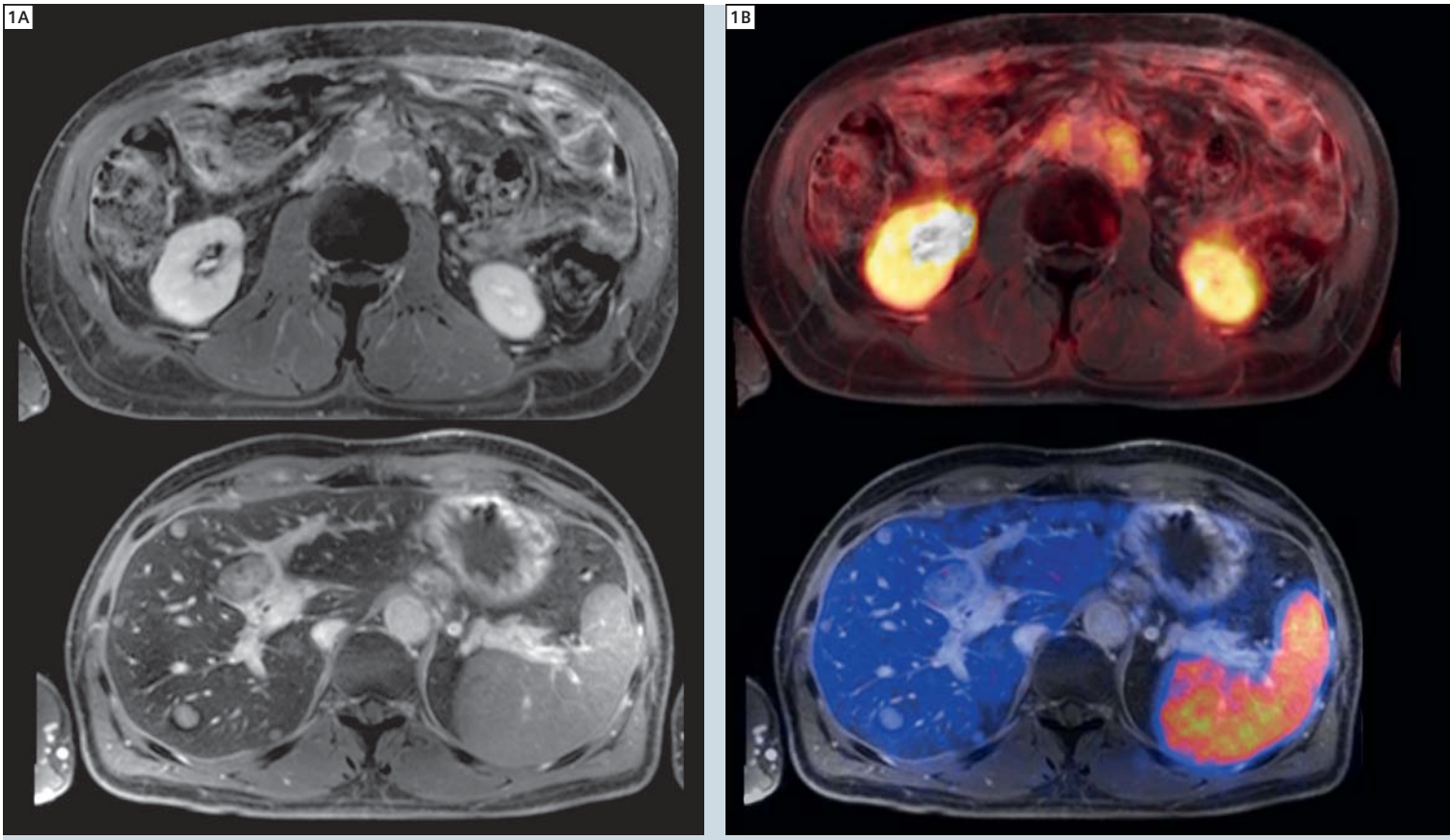

1A–B **1A**: Contrast-enhanced T1w 2D FLASH with fat saturation showing extensive retroperitoneal and hepatic tumor spread of the NET with partially necrotic areas. Corresponding DOTATATE PET in figure **1B**, acquired during simultaneous MR/PET, shows only slightly increased uptake/receptor upregulation of the retroperitoneal metastases and no focality within the liver.

Background

Much has already been written about the technology, the basic ideas as well as the potential clinical needs behind the combining of MR and PET. As with all new imaging methodologies, there is debate as to how much this technology is really needed (similarly, for example, with the availability of PET/CT) and the discussion regarding MR/PET in particular concerns the level of integration and, even more fundamentally, the question whether the simultaneity of MRI and PET acquisition is really required.

It should be pointed out that now that the MR/PET technology is available in the Biograph mMR, real simultaneous imaging with different methodologies is possible in a clinical setting for the first time – a clear paradigm shift in how we acquire information about patients and their diseases. The combining of functional information derived by MR and the possibility to influence PET information and vice versa is stimulating researchers worldwide and hopefully this will also clearly impact on how we provide biomarkers for therapy decisions throughout the continuum of patient care. But also from a purely clinical and very practical perspective, simultaneity

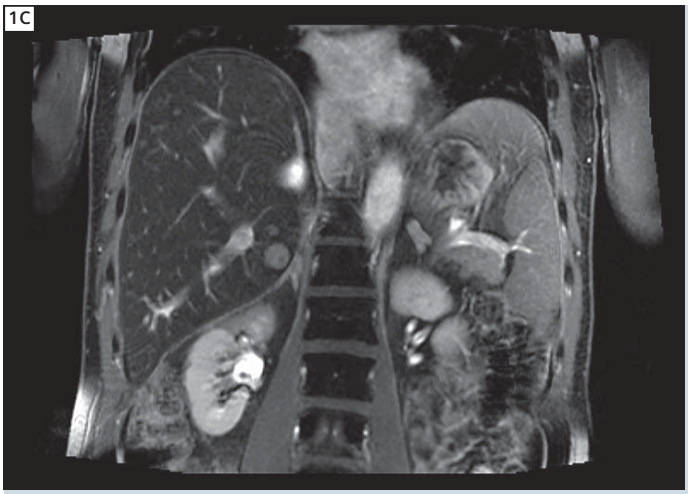

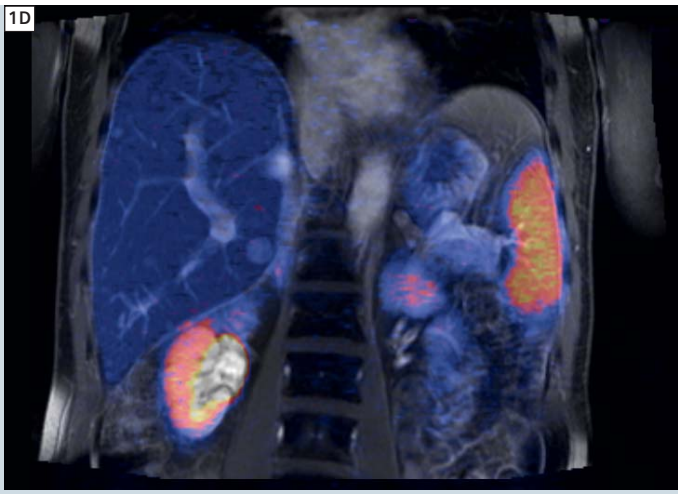

1C–D Corresponding coronal MR/PET.

of acquisition promises definite advantages over sequential acquisition – independently of how this sequential approach is organized (main concepts: a) different scanners and combination of results with software only, b) different scanners in different rooms with patient transport solution, or c) different scanners in the same room with patient transport solution). More detail about concepts and technology of MR/PET can also be found in the research supplement of the MAGNETOM Flash issue 3/2010 and in the MAGNETOM Flash issue 1/2011.

Impact of MRI on mMR imaging protocols

MRI has one main disadvantage when combining MR and PET in addition to not providing quantitative information about tissue density (a fact which has to be taken into account for attenuation correction of PET data): Data acquisition speed is limited compared, for example, to today's CT. MR imaging speed can of course be improved to some extent by increasing the strength of the B_0 field; by using different sequence techniques; by applying parallel imaging; and through its combinations (e.g. T2w 3D acquisition is only feasible within clinical routine as a turbo-spin-echo technique by the combination of variable flip angle evolutions with long echo trains and parallel imaging; *syngo* SPACE). In addition, the need for multiple contrasts and the capability to derive functional parameters like perfusion (T2* dynamics), cellularity (diffusion-weighted imaging, *syngo* REVEAL), microvessel density and permeability (T1w DCE; *syngo* VIBE or *syngo* TWIST for acquiring 4D data sets, *syngo* Tissue 4D for pharmaceutical modelling) are resulting in complex and relatively long examination times. For example, a comprehensive brain scan for tumor resection planning with MRI involves not only morphology scans (multiplanar T1w and T2w contrast including contrast media application) but possibly also fiber tracking and functional MRI to evaluate, for example, the tumor's involvement of essential areas like the motor cortex. An MRI exam that provides the required information can easily exceed half an hour and complex whole-body scans with MRI can easily take one hour.

Furthermore, these scans also generate a huge volume of imaging data. A standard whole-body MRI protocol in our clinical daily practice comprises 1,000 to 1,500 images; and this amount is increased dramatically by adding information from DWI, T1w DCE, etc. To provide another example of the level of complexity of these multimodal MRI approaches: A state-of-the-art prostate MRI exam aimed at local tumor staging / detection includes not only multiplanar / 3D high-resolution T2w TSE images but also T1w DCE, 3D MR spectroscopy, and DWI (including ADC calculations). Leaving aside the necessary post-processing, more than 2,000 images are acquired and have to be taken into account for diagnoses. But what does this mean to the simultaneously acquired PET data, and how is this influenced by such a relatively time-consuming and complex MRI exam?

In today's sequential PET/CT routine, PET can be regarded as a stand-alone imaging acquisition. CT (independent if only as a native low-dose or multi-phase contrast-enhanced scan) is acquired completely independently from the PET. Consequently, long PET measurement times are not desirable. Furthermore, the relatively small dimensions of the PET beds in a larger number of PET/CT scanners and physiological processes like filling of the bladder, bowel movement and uncomfortable patient fixation require the shortest possible PET scan times, in overall terms and per bed, especially also to limit the time-difference between the "snap-shot" CT (a whole-body scan with the latest CT generation can be done in less than 10 seconds at sub-millimetre resolutions) and the corresponding metabolic / PET information. As a further consequence of the time-constraints on PET measurements, dynamic

and late PET scans can be considered as wishful thinking and are not yet part of clinical routine, despite the promising results reported over recent years. This also applies to some degree to gated PET acquisition. Another problem is the relatively small number of patients included in these reports which makes it difficult to apply these techniques in daily patient care on a larger scale and thereby make economies of scale. But how do the relatively long MRI examination times, the need for complex functional information and the simultaneous acquisition of MR and PET data fit together? How will MR influence the PET acquisition and vice versa?

- The used PET detector for simultaneous MR/PET is characterized by a large field-of-view (in fact the largest available for clinical routine) which allows us to cover large areas if not the whole organ (brain, liver) in one go. Furthermore, the high sensitivity allows for fast PET scans per bed and in total. However, the relatively long MR imaging time and the high sensitivity of the detector results in an 'oversampling' of PET data, allowing gated PET scans (e.g. by adding information of the diaphragm movements derived from the simultaneous acquired MRI) or even longer dynamic PET acquisition when focusing on one organ. And whilst such an exam will take longer than a standard PET/CT, such a patient would have to undergo an MRI anyhow, and a dynamic PET scan would not really be possible in clinical routine for a PET/CT scanner aiming for a high patient through-put.
- PET information can be used to reduce the required amount of MR information; in fact, MR and PET point out different aspects of biology and so far it is more a question of diagnostic power of an individual biomarker and their combination that will determine the content of future MR/PET protocols. The 3D in-phase / opposed phase T1w sequence for attenuation correction will replace its counterparts in the MR protocol only in rare cases. Also, thanks to the 3D VIBE with Dixon technique, this is nowadays a simple one breathhold scan and does not really extend the overall scan time. Nevertheless, information derived from this MR sequence is of a diagnostic nature as it is for any low-dose attenuation CT scan for PET/CT.
- Of course, simultaneous MR/PET does offer multiple chances to improve PET performance, for example by adding information about perfusion information to dynamic PET data, or by allow for motion or volume correction. It is evident that these techniques are especially appealing for very specific PET tracers (e.g. for dementia evaluation) or for obtaining dedicated biological information for therapy adoption, for example the presence and adoption to hypoxic stress of tumor tissue.

Clinical examples
Study design and equipment

At a given point in time, all patients examined with the Biograph mMR are included in clinical studies. In the first phase, imaging capabilities of the system are evaluated to derive important information for advanced imaging protocols. We also want to compare the clinical performance of MR/PET with PET/CT for existing PET/CT indications. Because of the convincing results of the first phase of the clinical testing and after

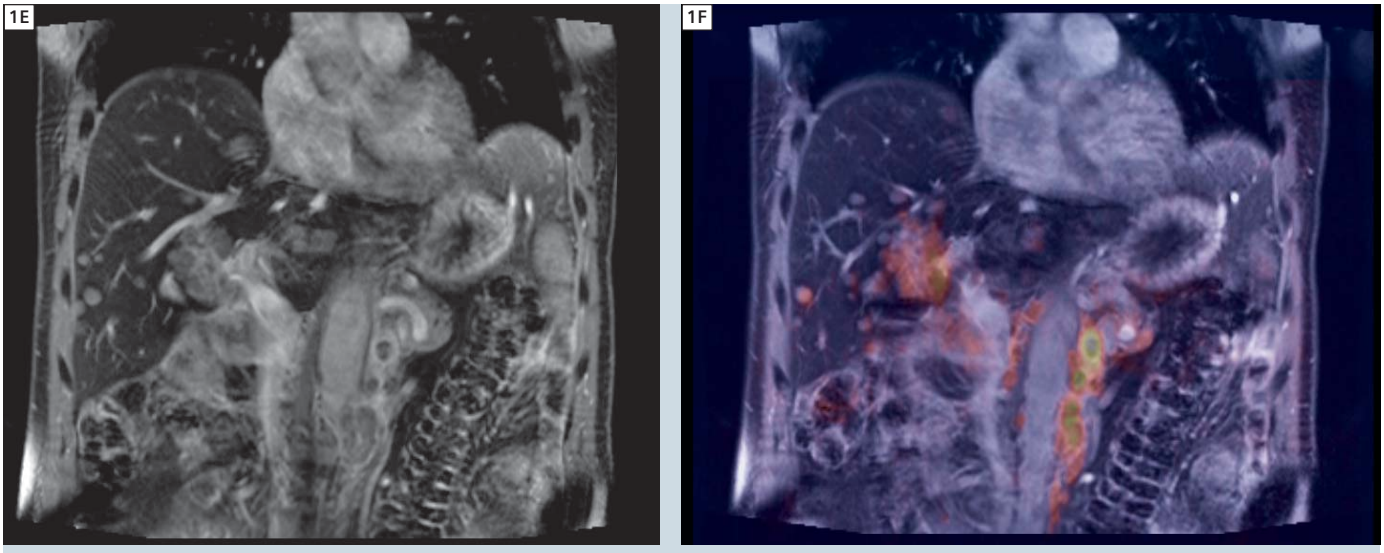

1E–F **1E** (MR only) and **1F** (b=800 s/mm^2 overlaid) show the extensive retroperitoneal tumor spread. In contrast to PET, DWI demonstrates areas with restricted diffusion as an expression of high cellularity which is not directly linked to the receptor expression but more to cell density. Not shown in this case are the quantitative ADC maps which are used to separate T2-shine through effects from real restriction of diffusion. These effects can both contribute to the signal in the original b-value images.

receiving the CE-label for the Biograph mMR, we expanded our IRB approval for the use of our system for imaging children* and now regularly use contrast-media for, for example, dynamic liver evaluations.

All patients have an indication for PET/CT and are scanned at the PET/CT and at the mMR. We apply body-weight adjusted PET tracers according to our clinical PET/CT protocols; the second scan is performed with the residual activity. Most of our patients received the PET/CT scan first. However, for some indications we now change this order. The installation of the Biograph mMR at our institution was the second world-wide, and the BrainPET prototype the first, used for advanced neuro-research and basic / methodology evaluation of the MR/PET technology. This scanner is placed in our radiopharmaceutical laboratories, which can produce all common radiopharamaceuticals in clinical imaging and research. The Biograph mMR is placed in a different building, but short delivery ways allow us to apply ^{11}C labelled tracers and other tracers than FDG within the framework of clinical pilot studies.

*MR scanning has not been established as safe for imaging fetuses and infants under two years of age. The responsible physician must evaluate the benefit of the MRI examination in comparison to other imaging procedures.

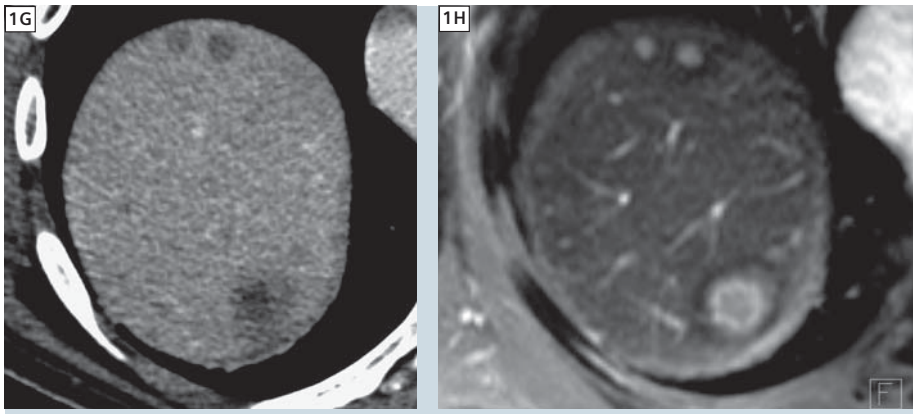

1G–H **1G**: Contrast-enhanced CT scan (late phase) and corresponding MRI in **1H** (contrast-enhanced late phase) show the superior soft contrast of MRI which enables detailed information about regional differences within the metastases.

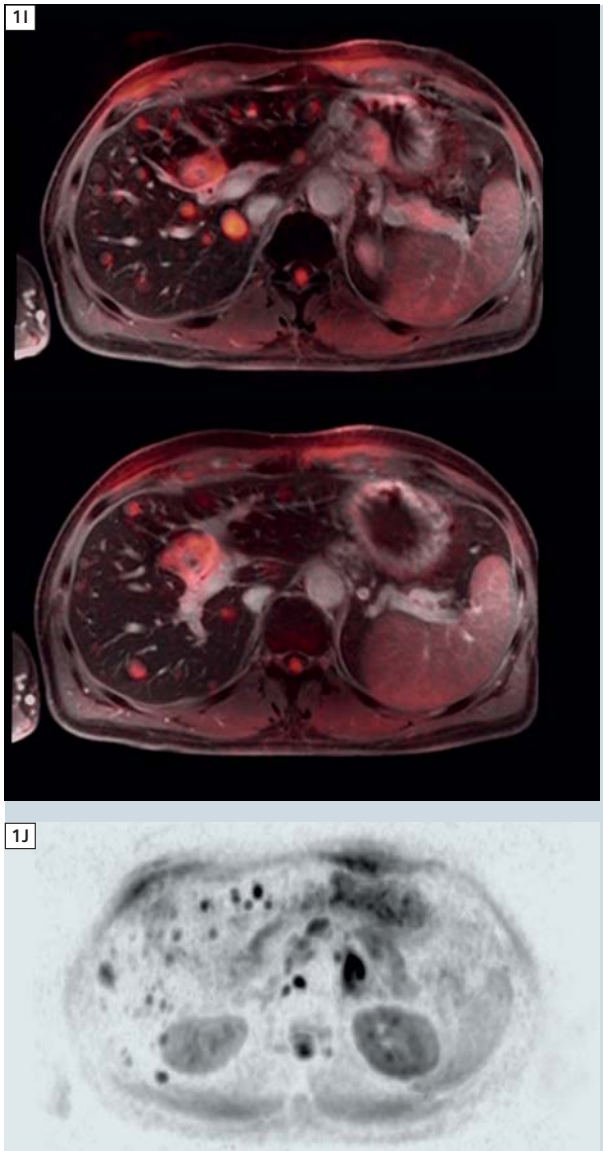

1I–J **1I** (DWI superimposed on contrast-enhanced T1w ce FLASH) and **1J** (thick-slice MIP of original b-value images) show the potential of DWI to provide detailed information about the total tumor load. Nevertheless, simply based on the original b-value images, a differentiation between tumor and reactive tissue, e.g. after surgery, as seen in the ventral abdominal wall, can be challenging. There is an additional finding of increased fat content of the liver.

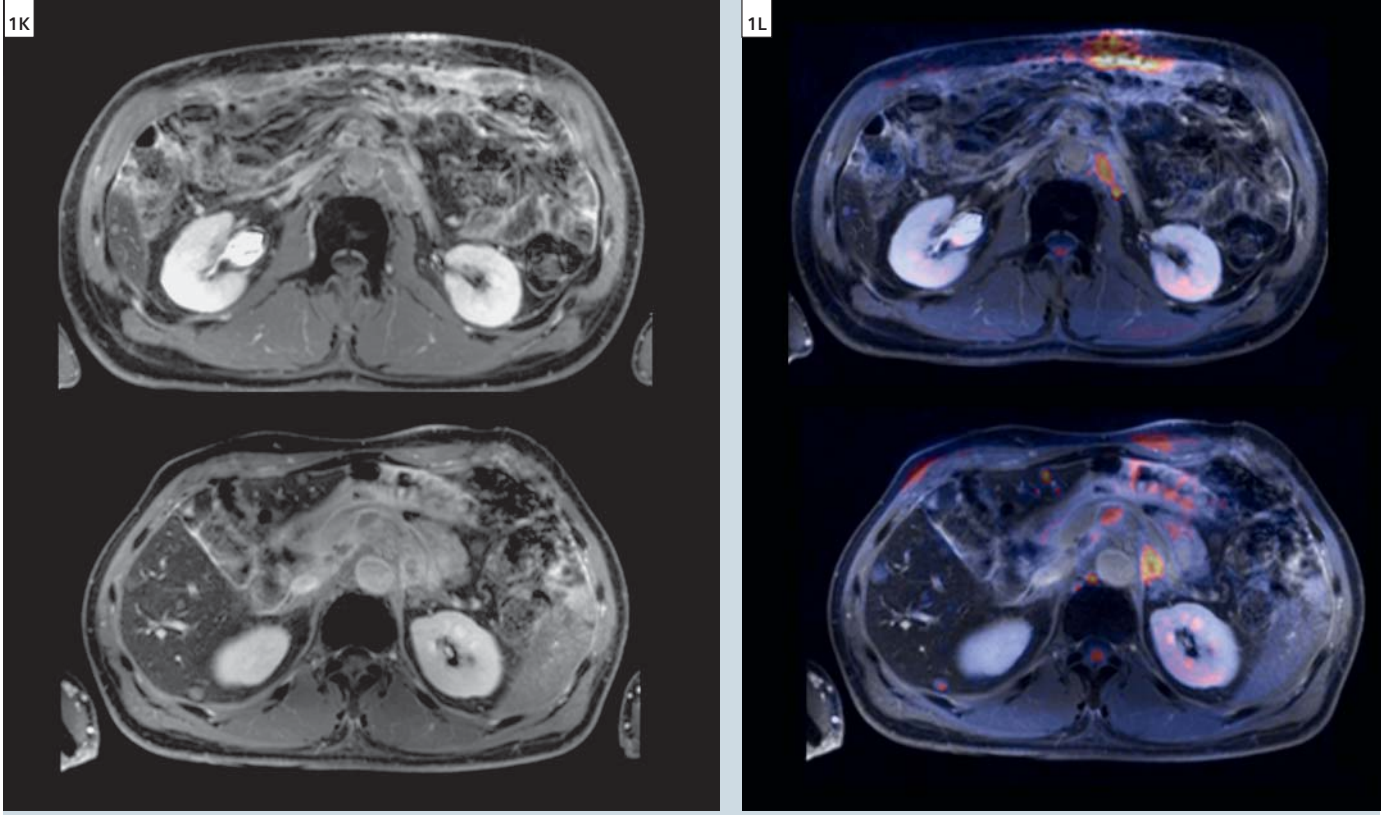

1K–L T1w contrast-enhanced MRI demonstrating extensive spread and involvement of paraortic lymph nodes stages with necrosis. In addition, diffuse enhancement of the peritoneum can be seen **(1K)**. Overlayed high b-value images do show however different aspects of metastases than T1w scan **(1L)**. Compare with figure 1B for evaluation of receptor status of the metastases.

MR/PET imaging protocols

We are now still in the evaluationary phase for different MR/PET protocols depending on clinical indications and patients' capabilities. In general, we try to focus more on clinically relevant combinations than to rigidly adhere to our imaging protocols. This approach can best be compared to the modules for whole-body MRI proposed by several working groups, which take into account clinical patterns of disease as well as the diagnostic power of MRI sequences, e.g. dynamic liver scans for colorectal cancers, coronal whole-body TIRM in case of high probability of bone metastases and FLAIR and post-contrast scans of the brain in case of lung cancer, etc., are added to a basic protocol. Our MR/PET protocols aim first at acquiring a comprehensive overview that is more comparable to conventional PET/CT and comprises basic MR sequences including the sequence for attenuation correction and then add a focused scan. Here we limit the scan range to smaller areas of interest and perform the specific MR protocols that also allow us to acquire dynamic PET data.
In the following case reports we describe two typical cases from our patient cohort. Both patients were scanned first with the PET/CT and then with the Biograph mMR.

Case 1
Evaluation of metastatic spread in case of a neuroendocrine tumor (NET)

This exam had to answer three important questions: First, what is the total tumor load; second, can this NET be treated by an internal radiotherapy; and finally, are there any complications that would cause an adoption of the therapy (e.g. recommendation of supportive actions in case of congestion of the biliary tract, obstruction of the urinary tract etc.). As one of the few clinical available 'therapeutics', ^{68}Ga DOTATATE was used in this patient. Over-expression of Somatostatine receptors of NET are a common finding. DOATATE has similar characteristics to DOTATOC and is used for imaging NETs. If labelled with ^{68}Ga, DOTATOC as well as the applied DOTATAE can be used as a tracer specific PET tracer to provide not only information about degree of receptor expression but also an evaluate the effectiveness of potential systemic ^{90}Y labelled DOTATOC/DOTATATE application for internal radiotherapy. However, as is the case for other tumors, metabolism and in this case receptor expression may vary not only between patients but also between different metastases of the same tumor within one individual. In addition, a common organ for metastastic spread of NET is the liver, but small filiae can easily be missed even when showing higher DOTATOC uptake because of the high background activity of liver tissue. Furthermore, since limited disease would potentially allow a more radical and curative approach e.g. atypical resection of liver metastases, a precise detection of filiae is essential for therapy assessment. It has been shown that MRI (using arterial phase of dynamic liver scans and / or diffusion weighted imaging) is the most accurate imaging method for an accurate evaluation of liver metastases of a NET. But DWI in particular also has

the potential to provide fast assessment of the total tumor load. By quantifying diffusion restriction it has already proved itself as an early therapy response biomarker for other tumor entities.

The images shown are from a 47-year-old male patient. With a weight of 82 kg and body height of 195 cm (BMI 21.56 kg/m^2), 167 mBq of ^{68}Ga DOTATATE was injected. After an uptake time of 20 min, a PET/CT was acquired including contrast-enhanced diagnostic CT scans and 78 min after tracer injection, the MR/PET examination was started (due to low residual activity, time per bed was 8 min, 3 beds were measured). PET/CT and MR/PET showed both multiple hepatic, coelical and retroperitoneal filiae of the known NET with only slightly increased receptor expression, most evident for the ceolical / retroperitoneal metastases. As expected, MRI could visualize more hepatic filiae and also allow for a more sensitive evaluation of diffuse reactions of the great omentum due to both advanced tumor spread and to the surgical approach before the patient was sent to our department. For the hepatic filiae, only discrete uptake could be seen in some larger metastases. However, this is not visible within the normal range of standard uptake values as used for images with overlaid PET; clear focal uptake is not seen and multiple metastases show no increased uptake compared to the liver background. As expected, the diagnostic performance of the PET/CT is inferior to MRI (MR/PET) but the information derived from MRI and DWI also show different aspects of tumor biology than PET; DWI reveals areas with higher cellularity that are not necessarily linked to a higher level of receptor expression.

Alongside the clinically comprehensive information derived from a combined MR/PET, this case shows clearly the high image quality achievable in challenging cases in the abdomen where MRI at 3T not only has the advantage of a high SNR but must also take into account potential negative effects. We do not apply to this patient the motion-freezing techniques which we also evaluate at our institution in a clinical setting. Motion-freezing and correction will unquestionably have an impact on diagnostic accuracy, especially for brain and liver MR/PET exams. However, in this clinical example no change of therapy would be evident: The extent of disease and the missing clear increase of uptake of the liver metastases compared to the residual normal liver parenchyma and the massive tumor load negates any further surgical approach.

Case 2
Evaluation of lung cancer

Lung cancer is perhaps the most evident indication for a PET/CT scan. MRI has not played a role in the diagnostic work-up so far, although the diagnostic accuracy of MRI has improved dramatically over recent years. The potential to detect small lung nodules is size-dependent but especially for the therapeutic relevant lesions with diameters >4 mm is comparable to state-of-the-art helical CT techniques. By adopting MR sequence techniques, lung MRI at 3T is clinical reality. Furthermore, MRI can add important information about, for example, infiltration of the chest wall, or provide detailed knowledge about vessel impairment which can be used for a detailed

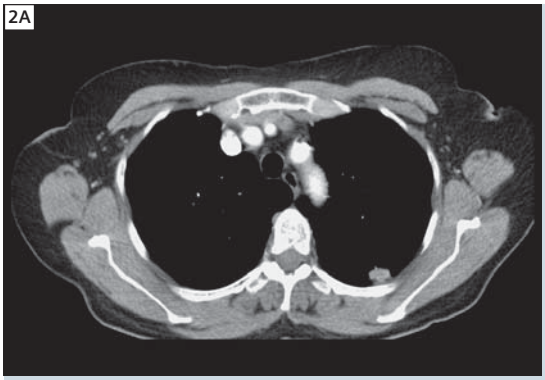

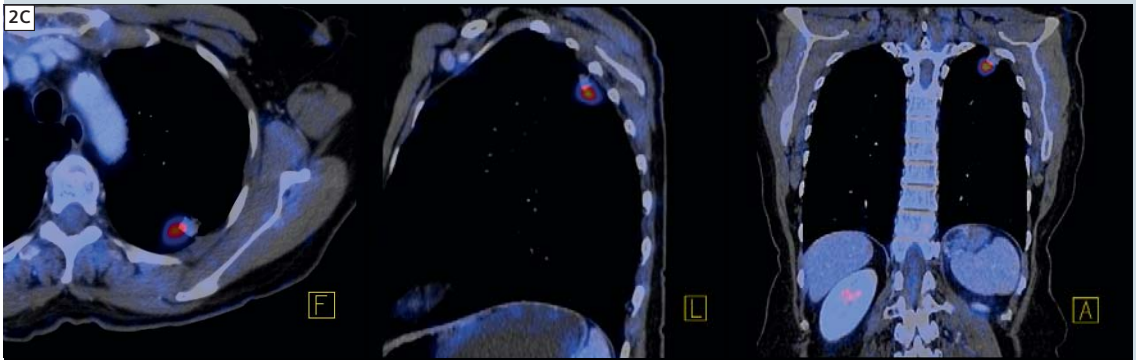

2A–C Contrast-enhanced CT scan (**2A** soft-tissue window and **2B** lung window) demonstrates the left apical lung nodule. As expected clear focal FDG uptake can be seen, however, fused on the contrast-enhanced diagnostic CT scan, a mismatch between PET (which is acquired during free breathing) and the cancer is seen in **2C**. However, fused on the native attenuation correction CT, this mismatch is as expected less evident (not shown).

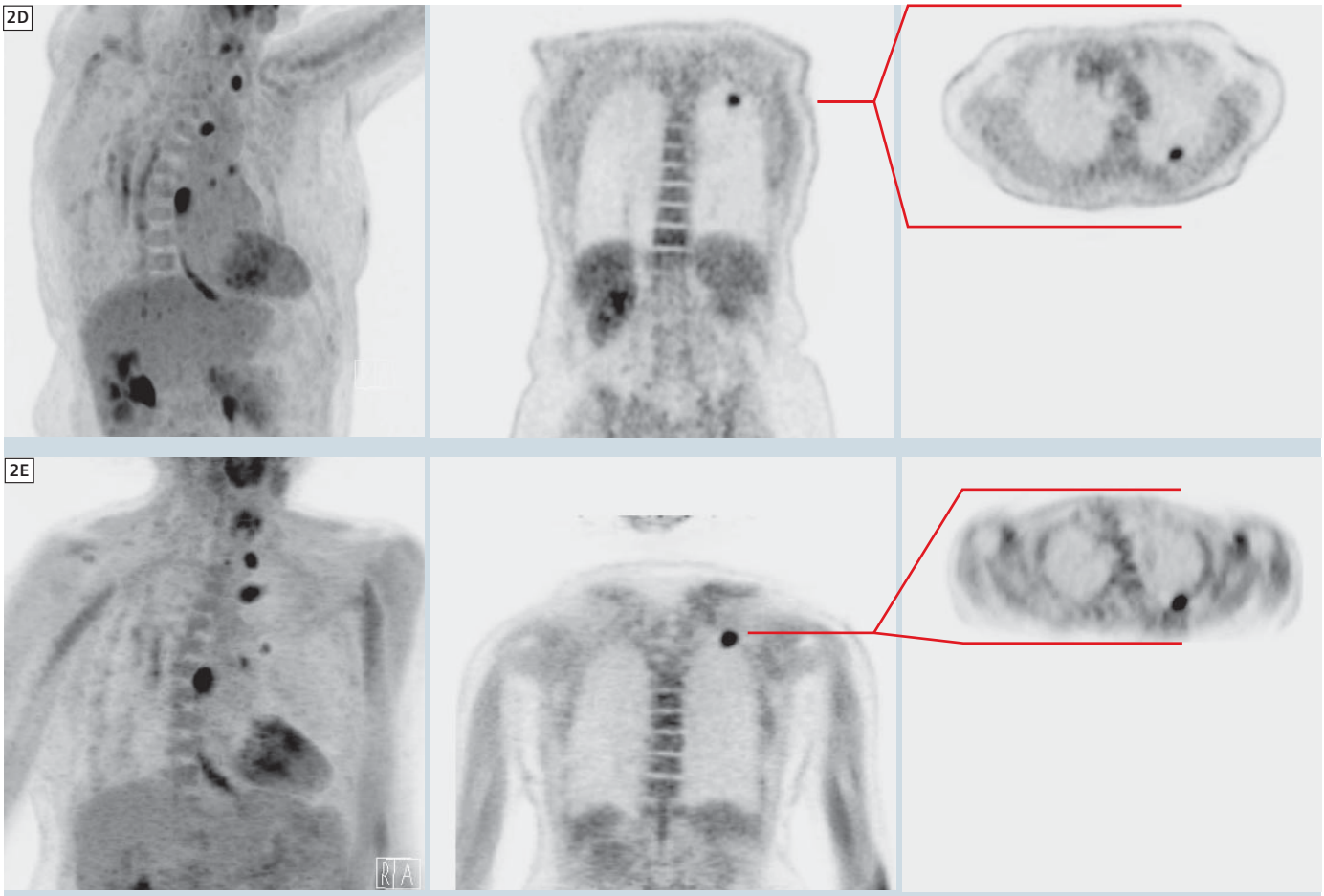

2D–E **2D** shows MIP and MPR of the PET derived from the PET/CT scan. Corresponding PET derived from the MR/PET in **2E**. Note that the MR/PET scan had to utilize the residual activity of the first acquired PET/CT. Note also that for MR/PET the arms can be positioned more comfortably without negative impact on image quality even if positioned outside the MRI's FOV. Findings details are given in the text.

surgical therapy assessment. In addition, MRI can provide functional parameters such as:

- cellularity by DWI,
- 3D motion patterns of the lesions by dynamic MRI (TrueFISP techniques, in development are sequences with radial k-space sampling schemes in combination with compressed sensing; evaluation of motion is feasible with CT, too, especially in an elderly patient undergoing radiotherapy this is a clinically realistic setting. However, especially for young female patients, additional radiation should be avoided)
- perfusion (again, radiation is a topic for CT scans when applied to young patients but also information derived especially by T1w DCE scans does differ from CT acquired perfusion data. DCE MRI was successfully applied to differentiate benign versus malignant lung lesions).

Especially in the evaluation of lung lesions of unknown origin in younger patients, MRI has to be considered as a clear alternative to conventional CT exams.

In this case, a 70-year-old female (weight 60 kg, height 165 cm, BMI 22,04 kg/m^2) – after injection of 381 mBq ^{18}F-FDG and an uptake time of 55 min – underwent a PET/CT, including multi-phase contrast-enhanced CT scans, for staging of a suspected lung cancer. The patient was than referred to our MR/PET unit. Simultaneous MR/PET was started 122 min after injection of FDG; PET acquisition time per bed was adapted to 6 min to compensate for the low residual tracer activity (2 bed positions were acquired which covered the whole thorax as well as the cervical region).

PET/CT and MR/PET showed both the left apical lung cancer neighbouring the pleura but without clear evidence of an affection of the thorax wall; also no signs of a pleural infiltration are seen. In addition, two small hiliar lymph nodes are present as well as paraoesphagel lymphnodes which were all rated as metastases because of their high and

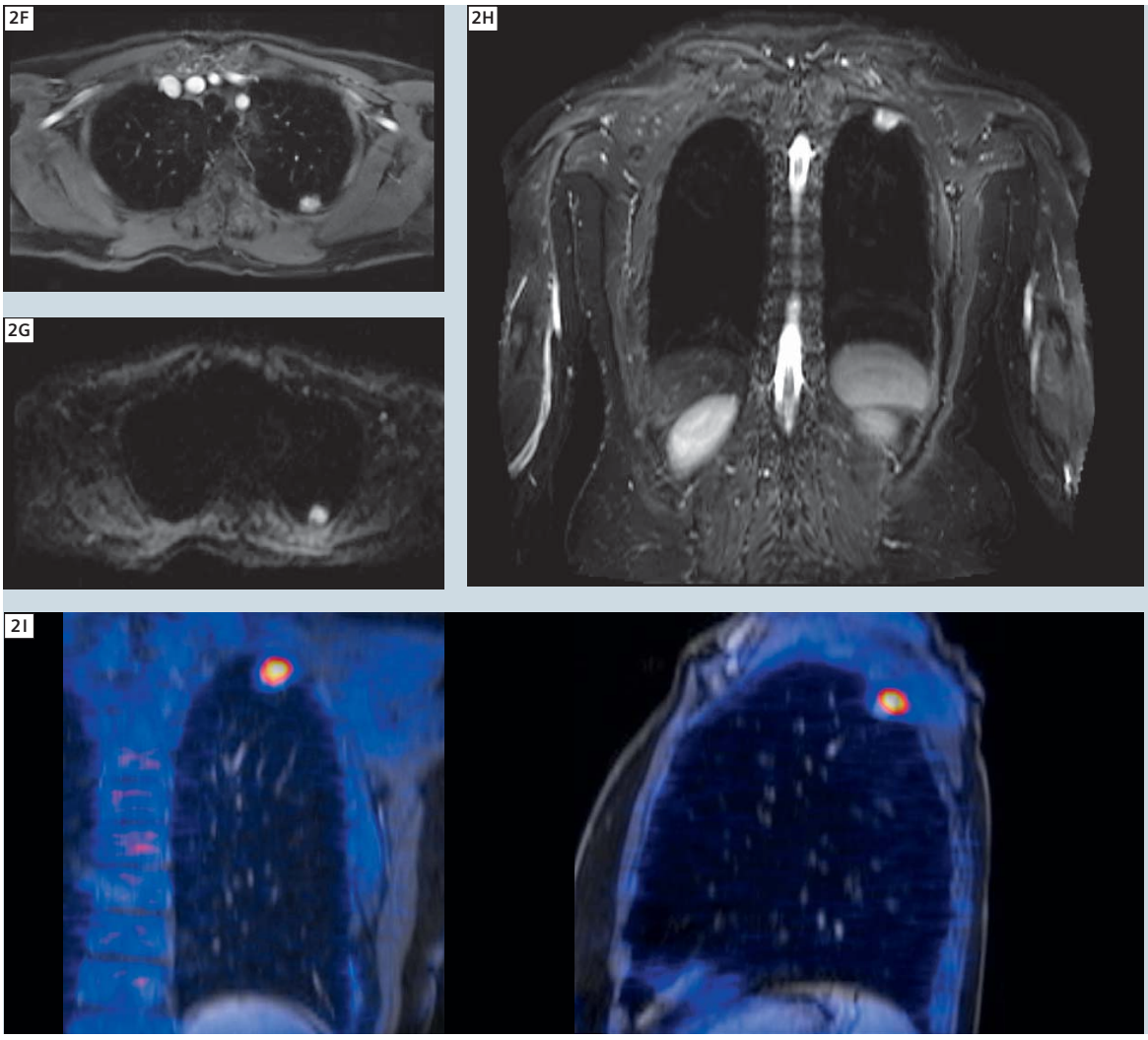

2F–I Transversal arterial phase T1w 3D VIBE scan is shown in **2F**. **2G** shows corresponding original b = 400 s/mm² DWI measurement. In **2H** coronal T2w STIR reveals the contact of the lesion to the very apical border of the pleura. Figure **2I** demonstrates focal uptake of the lesion also with the MR/PET examination. PET information is displayed with the simultaneously acquired contrast-enhanced 3D VIBE which demonstrates the high perfusion of the lesion.

focal FDG uptake. Both PET data sets also show a focal uptake within the oesophagus which has to be considered as a potential second malignoma. Both exams also demonstrate an increased but non-focal uptake of the lower oesophagus as often seen in case of recurrent inflammation which would also increase the possibility of a malignancy.

Another finding which corresponded to nodular formation in morphology was a small focal FDG uptake within the thyroid gland. Southern Germany is considered as an iodine-deficient area and therefore findings within the thyroid gland are common, however, a focal uptake within the gland can be linked also to thyroid cancer and a further evaluation of this finding is required, too.

Attenuation correction of PET data derived from the MR/PET examination is based on a segmentation approach. A direct comparison between of PET/CT and MR/PET is challenging in a clinical setting; different bio-distribution when measuring at different time-points is perhaps the main factor, but the problems associated with the measurement itself as well as different reconstructions of the PET images, etc., are also potential factors influencing the comparability of the two scans. With a SUVmax / SUVavg of 8.1 / 4.1 for the PET/CT and 8.8 / 4.3 for the MR/PET for the primary lung cancer lesion, a good correlation between the two scans is evident. However, it also shows that quantification of PET data is dependent on various factors which have to be taken into account, together with the error level that is deemed to be clinically acceptable, and these issues require an increased awareness especially from us clinicians.

This case clearly demonstrates that simultaneous MR/PET is clinically feasible at high quality and diagnostic accuracy, even where PET/CT would otherwise be considered as standard. MR/PET is a also a clear alternative for evaluation of lung lesions where radiation exposure is relevant, especially in young female patients. This clinical example comprises only basic MR techniques, but

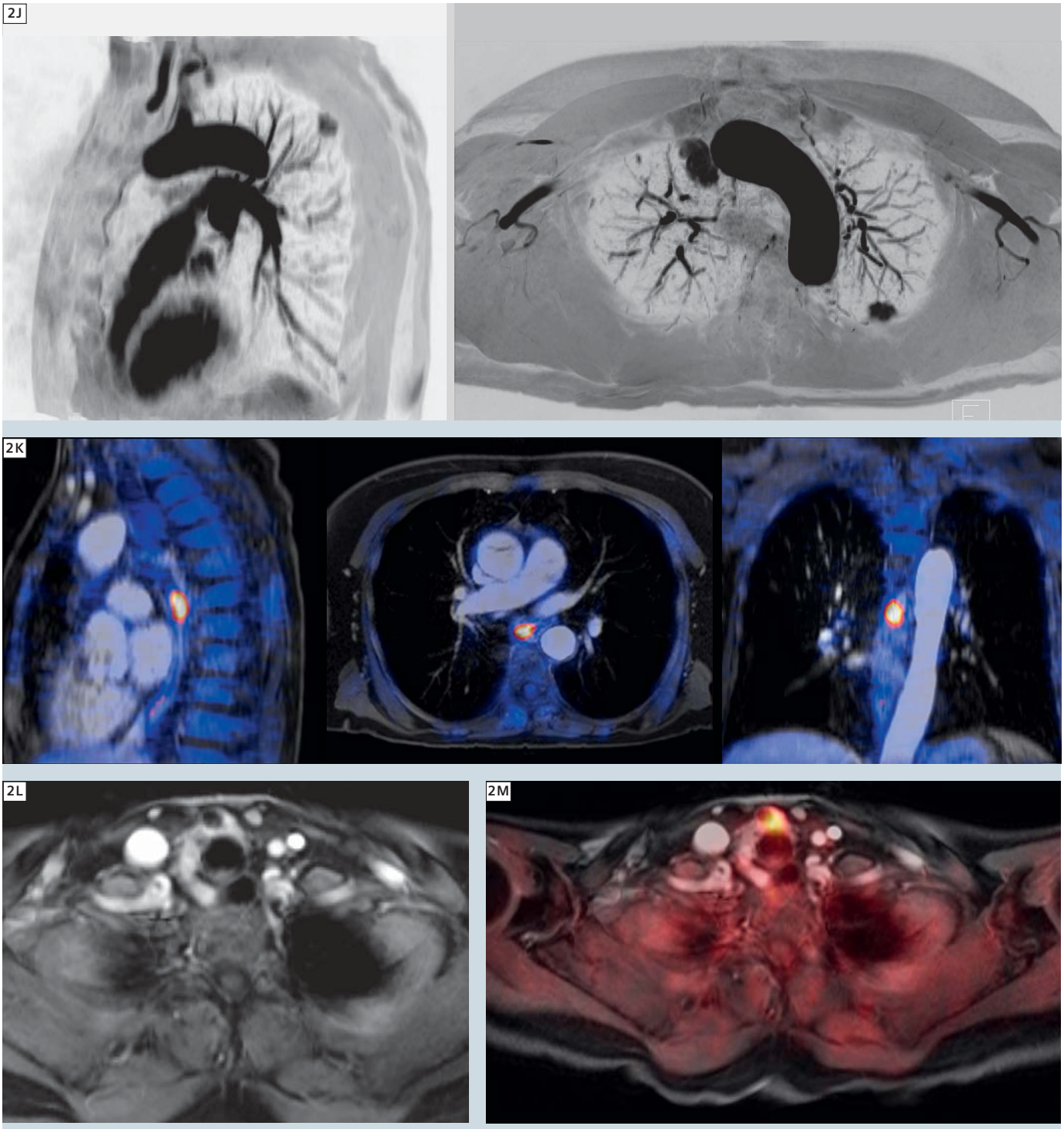

2J–M **2J** shows the relative relationship to the lung vessels. Images are thick-slice MPR and based on arterial phase 3D VIBE MR acquisition. In **2K** a multiplanar reconstruction based on the same MR sequence is shown, superimposed on the PET data and visualizing the focal uptake within the oesophagus of unknown origin. **2L** shows nodular changes within the thyroid gland and **2M**) superimposed with the PET the focal appearance of the increased FDG uptake in this area.

MRI can already deliver variable functional parameters. In this particular case, motion-freezing or correction would have been favourable but not clinically essential. However, especially for follow-up of small lung lesions, it has to be considered as an integral part of simultaneous MR/PET examinations.

Conclusion

As shown by the two cases in our ongoing clinical evaluation study, simultaneous MR/PET has already proven its potential to deliver outstanding image quality and offer all the advantages of MRI and PET in one examination. It is also evident that simultaneous MR/PET is about much more than just adding a radiation-free imaging modality to PET and that we have only begun to understand the clinical benefits of molecular MR. There is no doubt that it has huge potential to advance imaging in patient care and to provide detailed biomarkers for a vast range of diseases and therapies.

References

1 Thorwarth D, Henke G, Müller AC, Reimold M, Beyer T, Boss A, Kolb A, Pichler B, Pfannenberg C. Simultaneous 68Ga-DOTATOC-PET/MRI for IMRT treatment planning for meningioma: first experience. Int J Radiat Oncol Biol Phys. 2011 Sep 1 ;81(1):277-83. Epub 2011 Feb 6.

2 Werner MK, Brechtel K, Beyer T, Dittmann H, Pfannenberg C, Kupferschläger J. PET/CT for the assessment and quantification of (90)Y biodistribution after selective internal radiotherapy (SIRT) of liver metastases. Eur J Nucl Med Mol Imaging. 2010 Feb;37(2):407-8. Epub 2009 Dec 9.

3 Gehler B, Paulsen F, Oksüz MO, Hauser TK, Eschmann SM, Bares R, Pfannenberg C, Bamberg M, Bartenstein P, Belka C, Ganswindt U. [68Ga]-DOTATOC-PET/CT for meningioma IMRT treatment planning. Radiat Oncol. 2009 Nov 18;4:56.

4 Plathow C, Staab A, Schmaehl A, Aschoff P, Zuna I, Pfannenberg C, Peter SH, Eschmann S, Klopp M. Computed tomography, positron emission tomography, positron emission tomography/computed tomography, and magnetic resonance imaging for staging of limited pleural mesothelioma: initial results. Invest Radiol. 2008 Oct;43(10):737-44.

5 Plathow C, Aschoff P, Lichy MP, Eschmann S, Hehr T, Brink I, Claussen CD, Pfannenberg C, Schlemmer HP. Positron emission tomography/computed tomography and whole-body magnetic resonance imaging in staging of advanced nonsmall cell lung cancer-initial results. Invest Radiol. 2008 May;43(5):290-7.

6 Lichy MP, Aschoff P, Plathow C, Stemmer A, Horger W, Mueller-Horvat C, Steidle G, Horger M, Schafer J, Eschmann SM, Kiefer B, Claussen CD, Pfannenberg C, Schlemmer HP. Tumor detection by diffusion-weighted MRI and ADC-mapping--initial clinical experiences in comparison to PET-CT. Invest Radiol. 2007 Sep;42(9):605-13.

7 Judenhofer MS, Wehrl HF, Newport DF, Catana C, Siegel SB, Becker M, Thielscher A, Kneilling M, Lichy MP, Eichner M, Klingel K, Reischl G, Widmaier S, Röcken M, Nutt RE, Machulla HJ, Uludag K, Cherry SR, Claussen CD, Pichler BJ. Simultaneous PET-MRI: a new approach for functional and morphological imaging. Nat Med. 2008 Apr; 14(4) :459-65. Epub 2008 Mar 23.

8 Schraml C, Schwenzer NF, Martirosian P, Bitzer M, Lauer U, Claussen CD, Horger M. Diffusion-weighted MRI of advanced hepatocellular carcinoma during sorafenib treatment: initial results. AJR Am J Roentgenol. 2009 Oct;193(4):W301-7.

9 Boss A, Stegger L, Bisdas S, Kolb A, Schwenzer N, Pfister M, Claussen CD, Pichler BJ, Pfannenberg C. Feasibility of simultaneous PET/MR imaging in the head and upper neck area. Eur Radiol. 2011 Jul;21(7):1439-46. Epub 2011 Feb 10.

10 Pichler BJ, Kolb A, Nägele T, Schlemmer HP. PET/MRI: paving the way for the next generation of clinical multimodality imaging applications. J Nucl Med. 2010 Mar;51(3):333-6. Epub 2010 Feb 11.

11 von Schulthess GK, Schlemmer HP. A look ahead: PET/MR versus PET/CT. Eur J Nucl Med Mol Imaging. 2009 Mar;36 Suppl 1:S3-9.

12 Schlemmer HP, Pichler BJ, Schmand M, Burbar Z, Michel C, Ladebeck R, Jattke K, Townsend D, Nahmias C, Jacob PK, Heiss WD, Claussen CD. Simultaneous MR/PET imaging of the human brain: feasibility study.Radiology. 2008 Sep;248(3):1028-35.

13 Catana C, van der Kouwe A, Benner T, Michel CJ, Hamm M, Fenchel M, Fischl B, Rosen B, Schmand M, Sorensen AG. Toward implementing an MRI-based PET attenuation-correction method for neurologic studies on the MR-PET brain prototype. J Nucl Med. 2010 Sep;51(9):1431-8.

14 Wehrl HF, Judenhofer MS, Thielscher A, Martirosian P, Schick F, Pichler BJ. Assessment of MR compatibility of a PET insert developed for simultaneous multiparametric PET/MR imaging on an animal system operating at 7 T. Magn Reson Med. 2011 Jan;65(1):269-79.

15 Guérin B, Cho S, Chun SY, Zhu X, Alpert NM, El Fakhri G, Reese T, Catana C. Nonrigid PET motion compensation in the lower abdomen using simultaneous tagged-MRI and PET imaging. Med Phys. 2011 Jun;38(6):3025-38.

16 Catana C, Benner T, van der Kouwe A, Byars L, Hamm M, Chonde DB, Michel CJ, El Fakhri G, Schmand M, Sorensen AG. MRI-assisted PET motion correction for neurologic studies in an integrated MR-PET scanner. J Nucl Med. 2011 Jan;52(1):154-61.

17 Eiber M, Martinez-Möller A, Souvatzoglou M, Holzapfel K, Pickhard A, Löffelbein D, Santi I, Rummeny EJ, Ziegler S, Schwaiger M, Nekolla SG, Beer AJ. Value of a Dixon-based MR/PET attenuation correction sequence for the localization and evaluation of PET-positive lesions. Eur J Nucl Med Mol Imaging. 2011 Sep;38(9):1691-701. Epub 2011 Jun 18.

18 Delso G, Martinez-Möller A, Bundschuh RA, Ladebeck R, Candidus Y, Faul D, Ziegler SI. Evaluation of the attenuation properties of MR equipment for its use in a whole-body PET/MR scanner. Phys Med Biol. 2010 Aug 7;55(15):4361-74. Epub 2010 Jul 20.

Contact
Assoc. Professor Nina Schwenzer, M.D.
University of Tübingen
Department of Diagnostic and Interventional Radiology
Hoppe-Seyler-Straße 3
72076 Tübingen
Germany
nina.schwenzer@med.uni-tuebingen.de